DETAILED CHANGE DETECTION USING HIGH SPATIAL RESOLUTION FRAME CENTER MATCHED AERIAL PHOTOGRAPHY

Lloyd L. Coulter, Steven J. Lathrop, and Douglas A. Stow
Department of Geography
San Diego State University
San Diego, CA 92182-4493
lcoulter@geography.sdsu.edu
slathrop@rohan.sdsu.edu
stow@mail.sdsu.edu

ABSTRACT

Advances in computer and digital imaging technology have enabled the geospatial community to remotely view and analyze land cover and changes in land cover at very high detail. This paper explores the application of detailed change detection using precisely-registered, multitemporal digital aerial photographs. Six inch (0.15 m) spatial resolution color infrared aerial photographs were acquired along the San Diego County section of the U.S./Mexico border in May 2004 and July 2005. A technique referred to as frame center matching was employed during the flight, which enabled precise registration of the multitemporal image frames. Independent check points indicate that a registration root mean square error of 0.49 ft (0.15 m) was achieved. Multitemporal image overlay techniques were used to detect land cover changes associated with fire, development, illegal immigration, and border protection activity. The techniques presented enable the detection of fine-scale land cover changes for resource management.

INTRODUCTION

Image-based change detection is a common approach used for monitoring natural environments (Hobbs, 1990; Coppin et al., 2001; Hayes and Sader, 2001; Rogan et al., 2002; Coppin et al., 2004). Changes of interest for natural resources management and monitoring include: land cover and land use change; forest or vegetation change; forest mortality, defoliation, and deforestation; wetland change; forest fire; landscape change; and desertification (Lu et al., 2004). Due to the frequency of acquisition and the large area coverage per-scene, satellite imagery from Landsat Thematic Mapper (TM), Satellite Probatoire d'Observation de la Terre (SPOT), and Advanced Very High Resolution Radiometer (AVHRR) sensors have been widely used for change detection (Lu et al., 2004). However, imagery from these satellite sensors is too coarse to detect natural resource changes occurring on the scale of ten meters or less.

The size of land cover change features which may be detected through image-based change detection is limited by two factors: 1) the ground resolution element (or spatial resolution) of the multitemporal imagery and 2) the accuracy of spatial registration between the image sets (Stow and Chen, 2002). Large format aerial photography and high resolution satellite imagery from sensors such as IKONOS, QuickBird, and OrbView enable detailed imaging of natural resources and other land covers. However, achieving precise spatial registration (at the scale of individual pixels) between multitemporal image sets is costly and often impractical (Wang et al., 2005). Therefore, while detailed features may be detected using these types of high spatial resolution imagery, changes occurring at the scale of these detailed features are not likely to be detected due to misregistration between the images.

The objective of this paper is to explore the utility of precisely-registered, multitemporal digital aerial photographs for detecting land cover changes in the context of natural resources monitoring. A technique referred to as frame center matching was employed to acquire and accurately register very high spatial resolution, multitemporal aerial photographs. Resultant six inch (0.15 m) spatial resolution digital images were accurately registered within approximately one pixel. This level of spatial registration is remarkable, given the extreme and varied terrain of the sites investigated. The high spatial resolution and precise registration of the multitemporal image pairs enabled detection of change features such as individual shrub growth; individual shrub loss due to fire; vegetation recovery following fire, dirt road widening; off-road vehicle tracks; river channel change and sedimentation; new foot trails; small drainage scouring; individual tree removal; land clearing, and new dirt roads.

BACKGROUND

Spatial registration between multitemporal image sets is a critical requirement of per-pixel change detection and multidate image classification (Stow and Chen, 2002). Accurate registration of high spatial resolution imagery acquired from aerial platforms over areas of extreme relief is difficult and often unattainable using standard orthorectification or polynomial transformation algorithms. This is the case because polynomial warping models cannot account for the variable geometric distortions caused by terrain and commonly available digital elevation models (DEMs) lack the spatial resolution and elevation accuracy to properly orthorectify high spatial resolution imagery (e.g., 1 m) (Baker et al., 1995). This inability to generate precisely registered multitemporal data sets from high resolution imagery leads to significant change artifacts when performing change detection with this type of imagery (Dai and Khorram, 1998).

Achieving accurate spatial registration with airborne frame imagery is complicated by the wide view angles, and misregistration errors are often on the order of several pixels in areas of high and variable relief (Baker et al., 1995). Verbyla and Boles (2000) demonstrated that misregistration tends to overestimate total land cover change and that false changes resulting from comparison of multidate classifications are greater with a larger number of thematic classes. Misregistration within multitemporal image data sets ultimately results in a greater number of falsely detected changes and identification of fewer actual changes, degrading the change detection results.

Techniques can be employed during the acquisition of aerial imagery which may alleviate many of the complicating factors in image registration and change detection. An approach referred to as frame center matching for multitemporal image registration was utilized. The frame center matching approach is based upon matching camera stations in terms of horizontal position and altitude between multitemporal image acquisitions (Coulter et al., 2003). When image frames are captured with matched frame centers, parallax between the photographs (defined as the change in the relative position of a feature resulting from a change in viewing perspective (Lillesand an Kiefer (1994)) is minimized and images may be expected to exhibit the same terrain related geometric distortions (assuming that differences in camera attitude are negligible) (Coulter et al., 2003). The relative spatial position of frame center matched and non-frame center matched multitemporal image sets is illustrated in Figure 1.

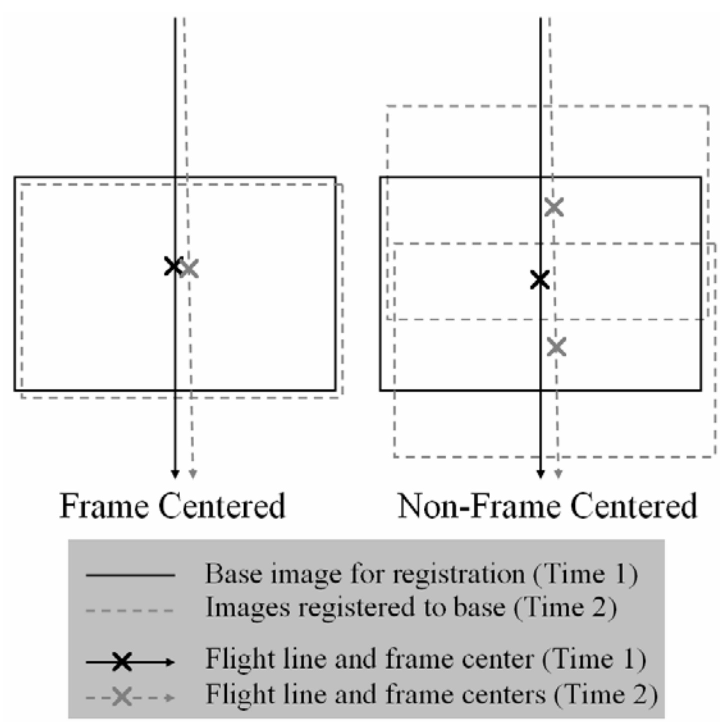

Figure 1. Position of frame center and non-frame center matched images relative to a registration base image.

Matching image stations is most effectively accomplished through the use of global positioning systems (GPS) to aid the pilot in maintaining the desired track and altitude, and automatically trigger image capture at the same camera station previously visited during the first multi-temporal pass. Four specific tools required for operational frame center matching using GPS data are:

1. Global positioning systems for logging and digitally archiving flight line and frame center coordinates for each image acquisition.
2. Flight planning software integrated with digital coordinates of flight line and frame coordinates from previous image dates.
3. In-flight, heads-up display enabling pilot to maintain flight line course and altitude (based on GPS coordinates).
4. Automatic triggering of image frames (based on digitally archived coordinates and in-flight GPS).

STUDY AREA

Change detection with precisely registered aerial photography was performed for a study area along the San Diego County, California portion of the U.S./Mexico border. Changes within this study area were reviewed at three sites: Marron Valley, Tecate, and Bell Valley. The study area is dominated by coastal sage scrub vegetation, with areas of southern mixed chaparral, chamise chaparral, and non-native grassland. The terrain within this area is characterized as mountainous, with an average elevation range of 300 m and an average slope of 10 degrees. A three-dimensional visualization of a typical site within the study area is given in Figure 2.

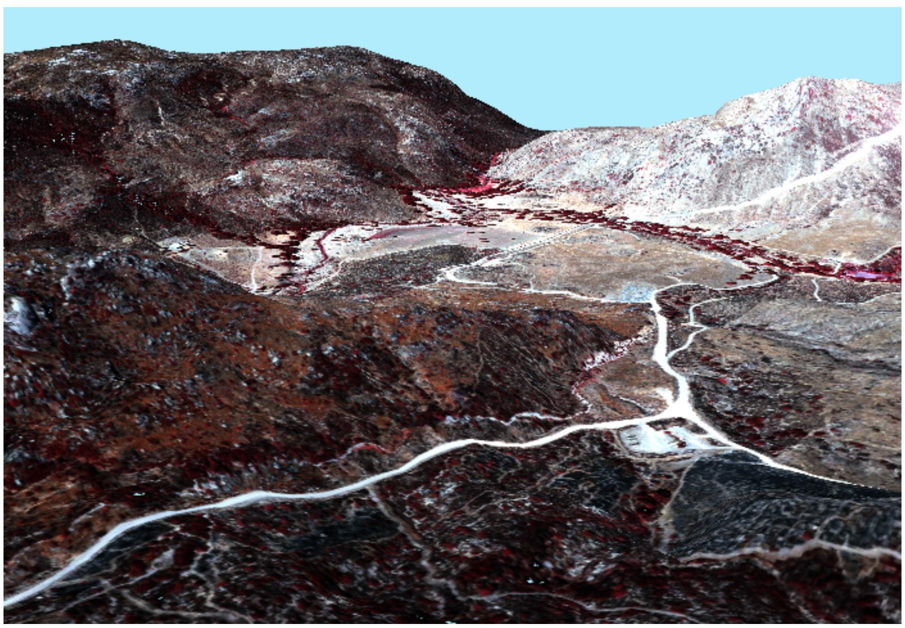

Figure 2. Three-dimensional view of Bell Valley showing the varied terrain within the U.S./Mexico border study area. The terrain vertical exaggeration is 150%.

DATA AND METHODS

Large format (9 inch by 9 inch) color infrared aerial photographs were acquired at a scale of 1" = 1000' (1:12,000) on 13 May 2004 and 22 July 2005 from a fixed wing aircraft. During the 13 May 2004 flight, standard (non-differentially corrected) GPS positions were recorded for each photo station as the aircraft flew a pre-determined flight path. These recorded GPS positions were later programmed in to the GPS-based navigation system for the 22 July 2005 flight, and the frame center matching technique previously described was employed to assist navigation of the aircraft down the previously flown flight path and trigger camera exposure at the same photo stations visited in May 2004. During the 22 July 2005 flight, the aircraft navigation was again based on non-differentially corrected GPS. Predetermined altitudes were matched on both flights using the aircraft altimeter.

The CIR film (Kodak 2443) was processed using Kodak AR-5 chemistry to develop the exposed film to transparent positives (diapositive film). The resulting individual photograph transparencies were scanned using a Vexcel 5000 UltraScan photogrammetric scanner. The scan resolution was 12.7 microns (approximately 2000 pixels per inch), which yielded pixels with a ground resolution element of approximately six inches (0.15 m). The scanned images provided three spectral wavebands of data for each photograph: green (500-600 nm), red (600-700 nm), and near-infrared (700-900 nm).

Scanned aerial photographs acquired on 13 May 2004 were orthorectified using Leica Photogrammetry Suite (LPS) software. Horizonal ground control was extracted from United States Geological Survey (USGS) Digital Orthophotographic Quarter Quadrangle (DOQQ) images. Vertical ground control was extracted from National Elevation Dataset (NED) 30 m digital elevation model (DEM) data. Approximately nine ground control points were sampled for each photograph, and tie points were automatically generated between photographs. A block solution was used for the triangulation.

Scanned aerial photographs acquired on 22 July 2005 were orthorectified using the LPS software. While vertical ground control was extracted from the same NED 30 m DEM, horizontal ground control for each individual photograph was extracted from the corresponding 2004 orthorectified image frame. Twenty five control points were sampled for each image frame. Each 2005 image frame was orthorectified individually, and a block solution was not used for the triangulation.

The registration accuracy between ten of the 2004 and 2005 image pairs was assessed using 16 independent check points per frame with the LPS software. The root mean square error (RMSE) of check points was summarized per frame. The registration RMSE provides a measure of overall positional offset between the multitemporal image pairs, and is computed using coordinates from corresponding ground features between the multitemporal image pairs and Equation 1.

$$\text{RMSE} = \sqrt{\frac{1}{n}\sum_{i=1}^{n} \Delta X_i^2 + \Delta Y_i^2} \qquad (1)$$

Where:
n = the number of check points
i = check point (CP) number
ΔX_i = the X misregistration distance for CP_i
ΔY_i = the Y misregistration distance for CP_i

To analyze change between 2004 and 2005, multidate overlay composite images were generated by viewing the red waveband image layers from the 13 May 2004 and 22 July 2005 orthorectified photographs in separate color planes. The 13 May 2004 red waveband was displayed in the blue and green color planes, while the 22 July 2005 red waveband was displayed in the red color plane. Using this technique, features exhibiting a change in red waveband brightness appear red if the brightness increased between 2004 and 2005 or cyan if the brightness decreased between 2004 and 2005. Areas of no-change appear as gray-scale. Land cover changes were identified through visual inspection of the overlay composite images. Review of these changes illustrates the utility of high spatial resolution, frame center matched imagery.

Radiometric adjustments to correct for vignetting, hot spots (localized specular reflection of solar radiation from the surface to the sensor), and solar illumination differences were not applied to the scanned and orthorectified images and advanced change detection processing was not applied. Some brightness differences associated with varying solar illumination angles at the time of acquisition were noted between the registered image pairs. However, change detection results obtained using red waveband overlay composites are sufficient to illustrate the utility of high spatial resolution, precisely-registered multitemporal imagery for detecting detailed changes in land cover for natural resources monitoring.

RESULTS

Precise registration between the 2004 and 2005 frame center matched aerial photographs was achieved. Independent check points of the registration accuracy between ten of the 2004 and 2005 aerial photograph pairs indicate an average registration RMSE of 0.49 ft (0.15 m). The maximum RMSE was 0.7 ft (0.21 m), and the minimum RMSE was 0.33 ft (0.10 m). Therefore, spatial registration between the multitemporal image pairs is on the order of one six inch (0.15 m) pixel.

The high spatial resolution and precise registration of the multitemporal images enabled the detection of detailed changes occurring on the scale of feet to meters. A range of land cover changes apparent on red waveband overlay composite images (hereafter referred to as change composite images) are given in Figures 3 to 8. Examples of road disturbances to the landscape are shown in Figure 3. Large dirt road cuts through coastal sage scrub vegetation are shown in Figure 3a. The removal of vegetation between 2004 and 2005 resulted in an increase in brightness for these areas, and the cuts appear as red. Figures 3b and 3c illustrate the utility of precisely-registered, high resolution imagery for detecting widening of dirt roads. Also apparent in Figure 3b is a new foot trail which trends north/south and areas of increased (red) and decreased (cyan) soil exposure.

Vegetation disturbances associated with fire, possible tree mortality, and sedimentation in a low lying area along a creek are given in Figure 4. In the fire example (Figure 4a), the removal of individual shrub canopies by the fire is apparent (red in change composite). A decrease in the width of the dirt road is also evident (cyan in change composite). Figure 4b illustrates a reduction in overall tree canopy associated with tree mortality or possibly human intervention. The increase soil exposure under the tree yields a bright red color on the change composite image. Figure 4c illustrates what is likely to be sedimentation in a previously vegetated area (red in change composite), as well as increased ground cover in the surrounding riparian area (cyan in change composite).

Vegetation disturbances associated with human activity and drainage scouring are given in Figure 5. Figure 5a shows the detection of new trails and general vegetation disturbance associated with foot traffic through a grassland area (red color in change composite). Also apparent is decreased soil exposure (cyan in change composite) in the south east corner of the image, which may indicate a reduction in use of that section of trail. The impact of off road vehicle activity can be seen in Figure 5b. In addition, the increased use of a trail paralleling the road is apparent. Figure 5c shows the impact of water scouring a drainage and washing out a section of dirt road. The scoured vegetation appears red in the change composite. Shadowing at the road cut and the occurrence of a new shrub in the washed out portion of the road appear as cyan.

The detection of shrub canopy growth is shown in Figure 6. The precise registration of the multitemporal aerial photographs is best demonstrated in Figure 6a, where growth of an individual shrub canopy is detected in the change composite image. The decrease in soil exposure by the vegetation canopy results in a cyan color in the change composite image. The width of new growth on any single side of the canopy is approximately 0.5 m. Figure 6b shows the increase in canopy cover of riparian shrubs between 2004 and 2005 (cyan in change composite). Likewise, Figure 6c shows the detection of new vegetation covering a sand bar in 2005. Red coloration across the remainder of the area in Figure 6c is associated with radiometric differences between the two photographs caused by differences in the time of day of the acquisition.

Figure 7 illustrates the detection of vegetation recovery and an example of how invasion by non-native plants within a drainage may be detected. Detection of vegetation recovery following fire is shown in Figure 7a. Cyan coloration in the change composite image generally corresponds with increased vegetation cover following recovery, while red coloration corresponds with further canopy die-back following the fire or increased soil exposure. Inclusion of data from the near-infrared wavebands with advanced change detection methods would result in more accurate identification of the recovered tree canopies; however, this was beyond the scope of this study. Figure 7b illustrates the detection of vegetation recovery from a dirt road cut, and the decreased soil exposure is indicated in cyan in the change composite image. Figure 7c provides an example of how an invasion by a non-native plant may appear in a red waveband color composite change image. An area with increasing herbaceous cover between 2004 and 2005 is clearly highlighted in cyan.

Land cover changes due to development are illustrated in Figure 8. Figure 8a shows a site that has changed from under construction to developed. Decreases in red waveband brightness due to pavement and landscaping are apparent, as well as increases in red waveband brightness likely due to a change in surface soil type. Detailed changes such as the addition of boulders in the landscaping were also detected. Figure 8b shows the impact of a radio tower installation

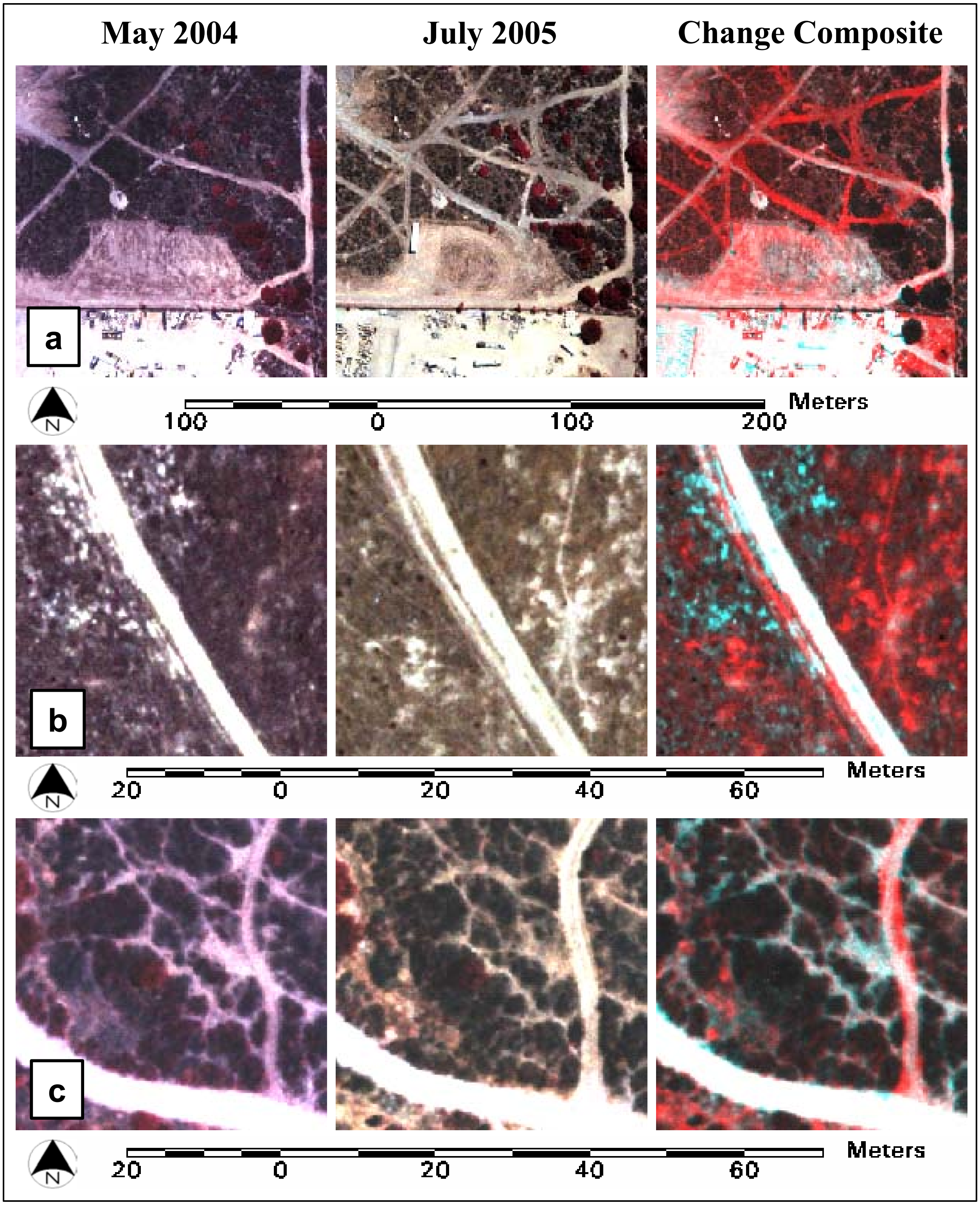

Figure 3. Road disturbances to the landscape. May 2004 and July 2005 color infrared images are displayed. The change composite is a red waveband overlay composite image, where red coloration indicates increase brightness over time and cyan indicates brightness decreasing over time.

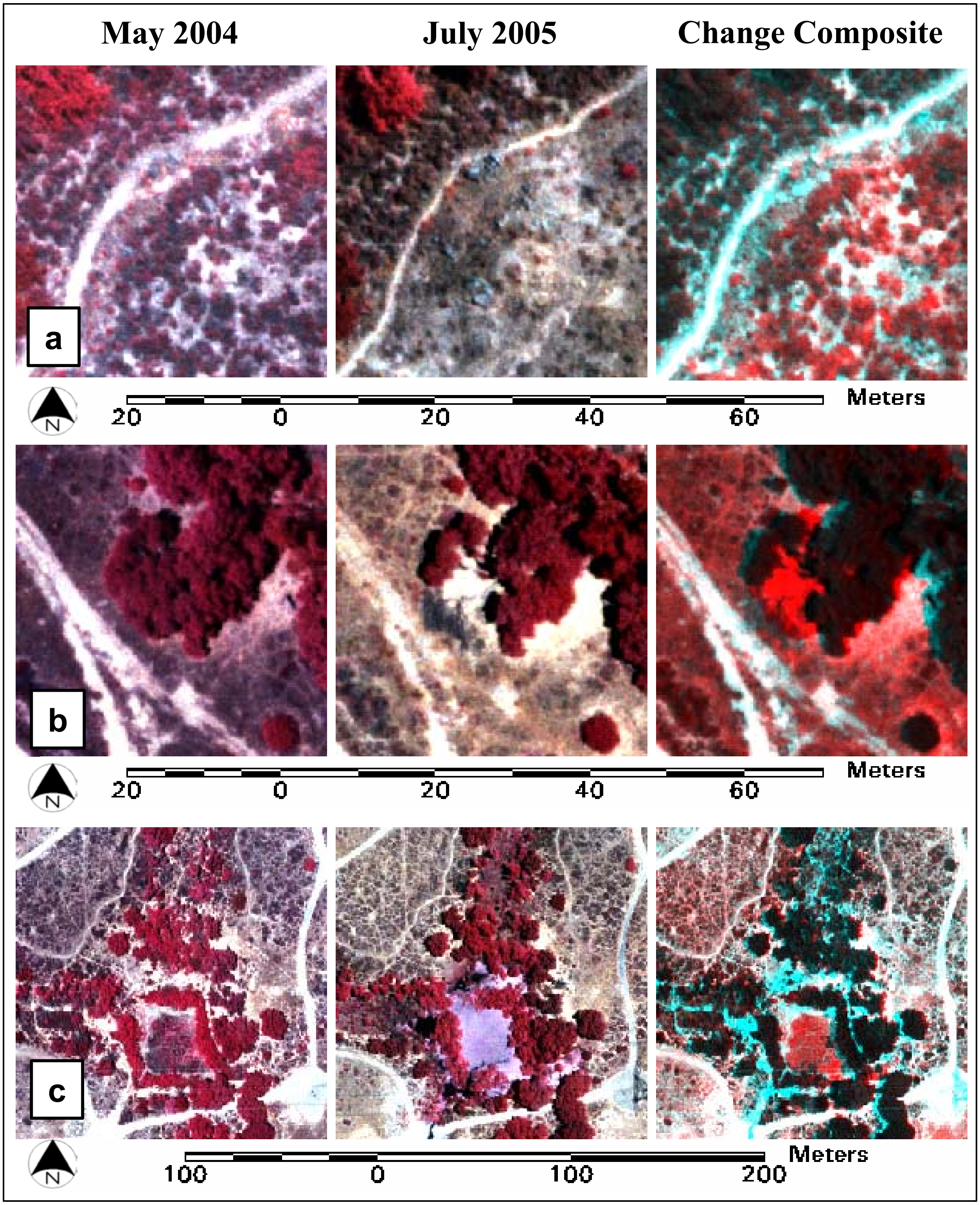

Figure 4. Natural vegetation disturbances. May 2004 and July 2005 color infrared images are displayed. The change composite is a red waveband overlay composite image, where red coloration indicates increase brightness over time and cyan indicates brightness decreasing over time.

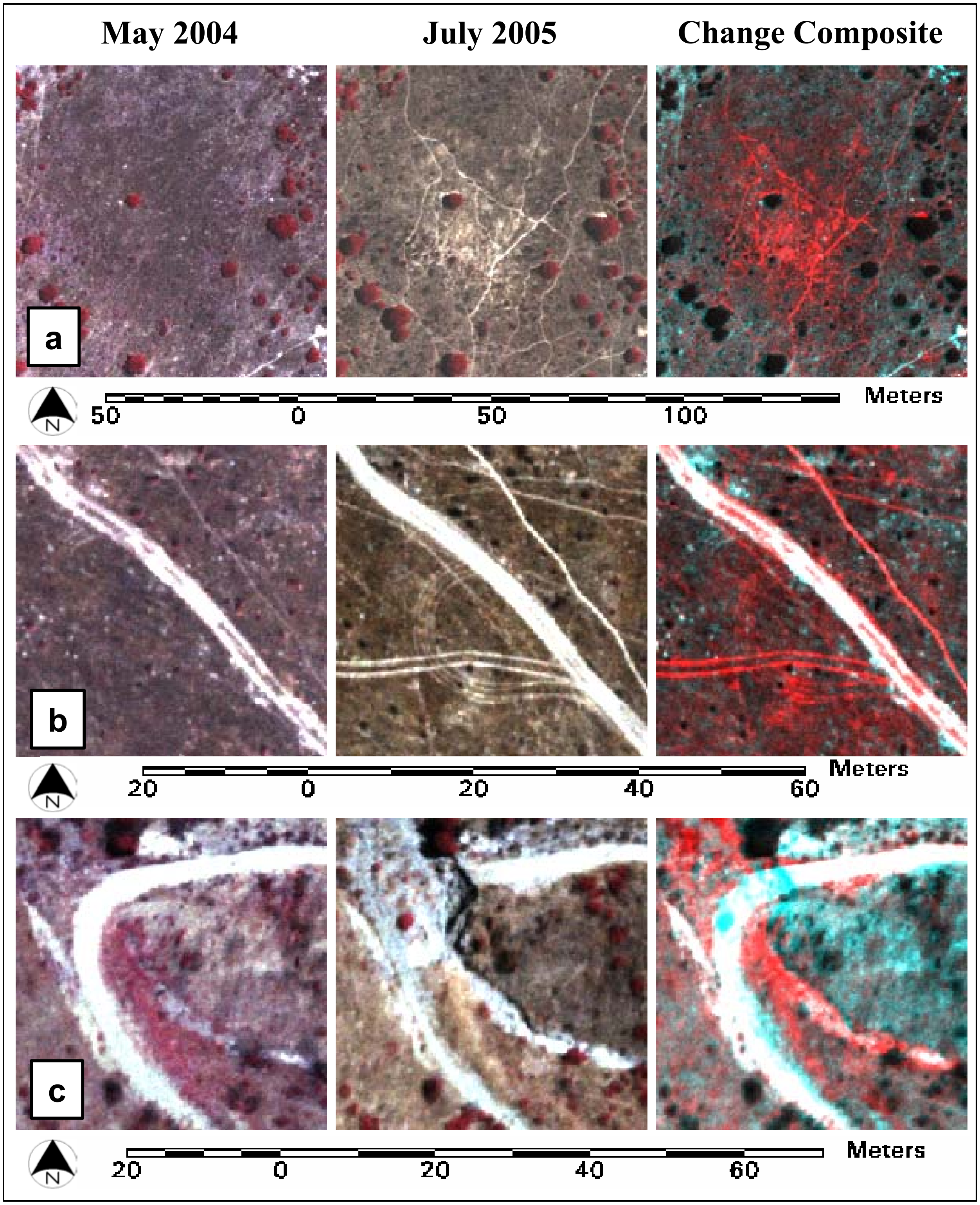

Figure 5. Human and natural vegetation disturbances. May 2004 and July 2005 color infrared images are displayed. The change composite is a red waveband overlay composite image, where red coloration indicates increase brightness over time and cyan indicates brightness decreasing over time.

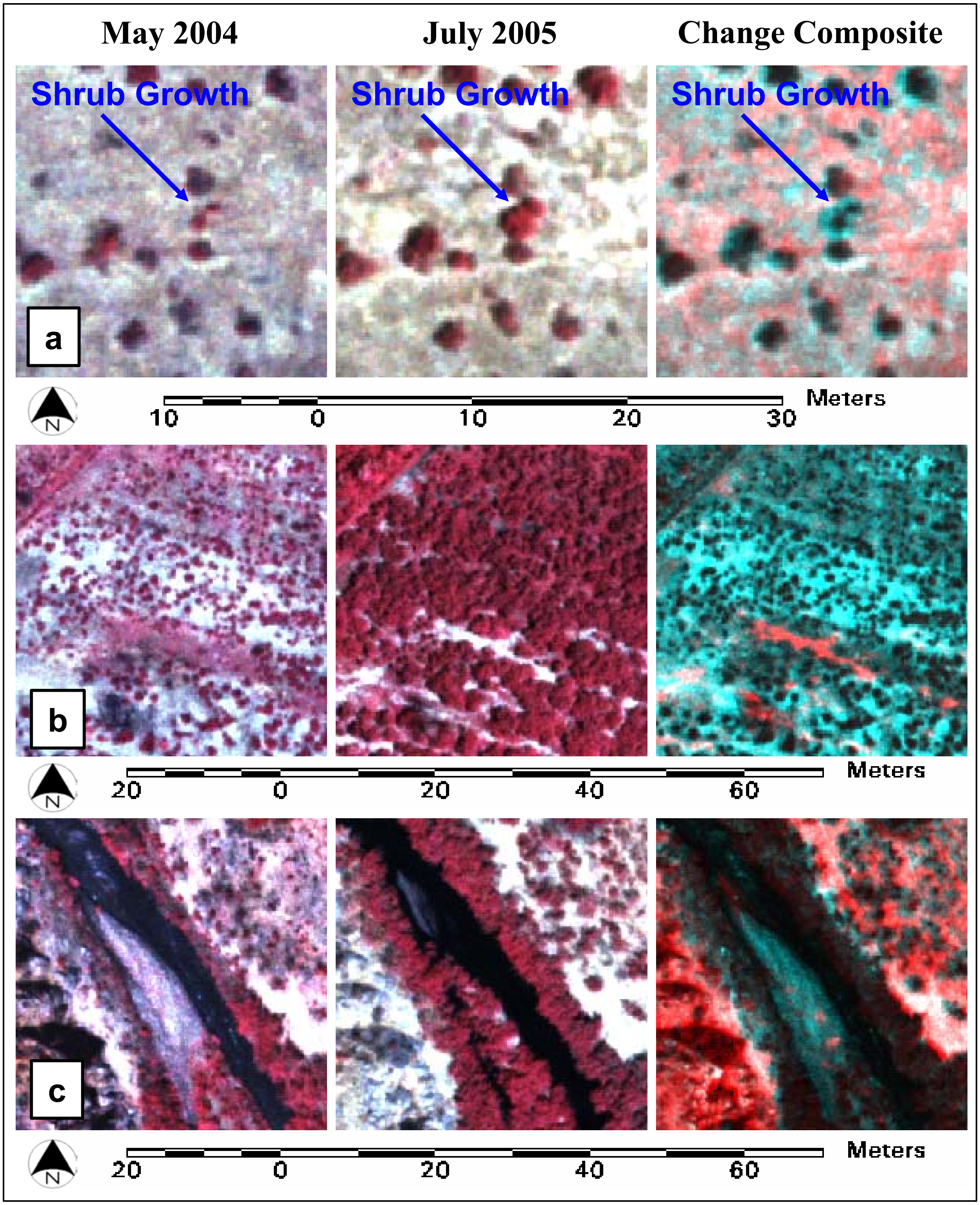

Figure 6. Vegetation growth. May 2004 and July 2005 color infrared images are displayed. The change composite is a red waveband overlay composite image, where red coloration indicates increase brightness over time and cyan indicates brightness decreasing over time.

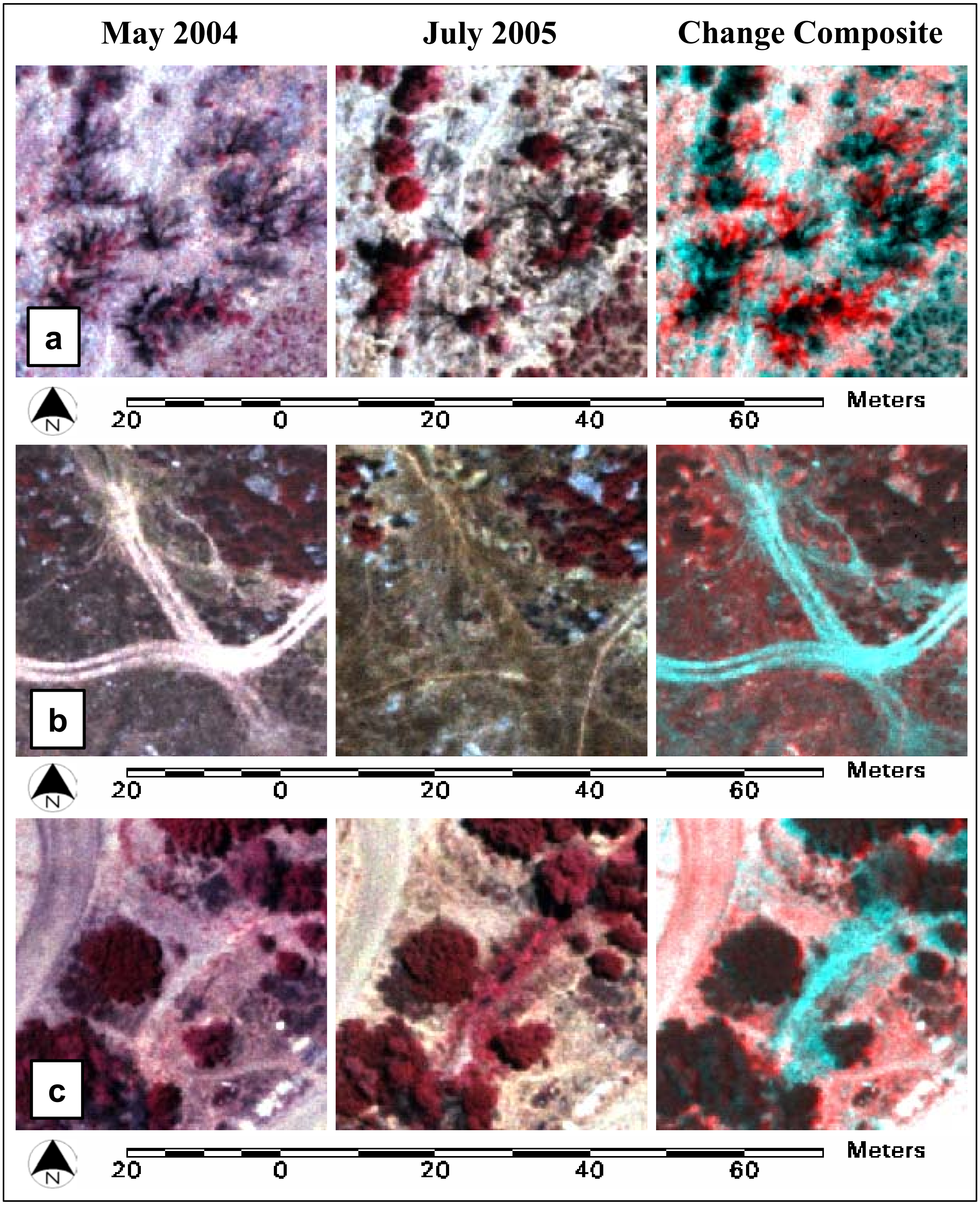

Figure 7. Vegetation recovery and non-native plant invasion. May 2004 and July 2005 color infrared images are displayed. The change composite is a red waveband overlay composite image, where red coloration indicates increase brightness over time and cyan indicates brightness decreasing over time.

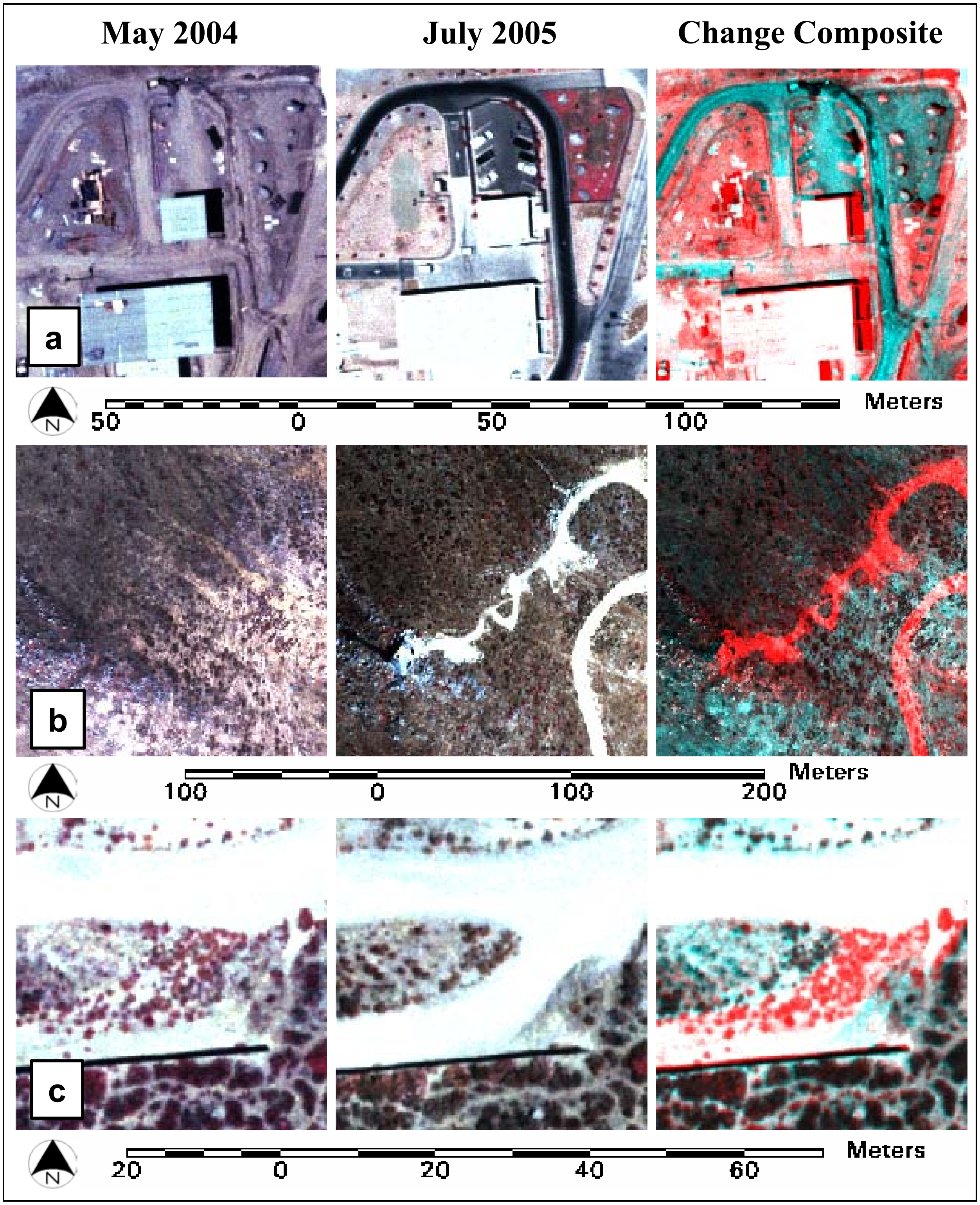

Figure 8. Development changes and disturbances. May 2004 and July 2005 color infrared images are displayed. The change composite is a red waveband overlay composite image, where red coloration indicates increase brightness over time and cyan indicates brightness decreasing over time.

and the associated access road. The tower is at the end of the road and casts a shadow to the northwest in the July 2005 image. Figure 8c shows the expanded use of an access road adjacent to the border fence along the U.S./Mexico border. Individual shrubs that were removed are detected in the change composite image.

CONCLUSIONS

Monitoring natural resources through image-based change detection requires precise registration between multitemporal imagery. The frame center matching approach to image acquisition and registration enabled accurate registration of very high resolution, multitemporal images in a area along the U.S./Mexico border with mountainous terrain. A simple change detection approach using color overlay composites illustrated the utility of precisely registered, multitemporal imagery for detecting detailed, small area land cover changes germane to natural resources management and monitoring. Land cover changes occurring on a scale of less than one meter were detected.

While a simple change detection procedure was employed here for demonstrative purposes, advanced image processing procedures are required to create a change map using multitemporal aerial photography. These include radiometric corrections for effects such as vignetting, hot spots, and solar illumination difference, and radiometric normalization of brightness values between dates. In addition, advanced image classification procedures exploiting the multispectral nature of color infrared imagery are necessary to categorize the types of changes occurring. These may include classification and post-classification comparison, change vector analysis, multidate classification, and multitemporal spectral mixture analysis.

REFERENCES

Baker, W., J. Honaker, and P. Weisberg (1995). Using aerial photography and GIS to map the forest-tundra ecotone in Rocky Mountain National Park, Colorado, for global change research. *Photogramm. Eng. Remote Sensing*, 61(3):313-320.

Coppin, P., K. Nackaerts, L. Queen, and K. Brewer (2001). Operational monitoring of green biomass change for forest management. *Photogramm. Eng. Remote Sensing*, 67(5):603-611.

Coppin, P., I. Jonckheere, K. Nackaerts, and B. Muys (2004). Digital change detection methods in ecosystem monitoring: a review. *Int. J. Remote Sensing*, 25(9):1565-1596.

Coulter, L., D. Stow, and S. Baer (2003). A frame center matching technique for precise registration of multitemporal airborne frame imagery. *IEEE Trans. Geosci. Remote Sensing*, 41(11):2436-2444.

Dai, X. and S. Khorram (1998). The effects of image misregistration on the accuracy of remotely sensed change detection. *IEEE Trans. Geosci. Remote Sensing*, 36(5):1566-1577.

Hayes, D. and S. Sader (2001). Comparison of change detection techniques for monitoring tropical forest clearing and vegetation regrowth in a time series. *Photogramm. Eng. Remote Sensing*, 67:1067-1075.

Hobbs, R. (1990). Remote sensing of spatial and temporal dynamics of vegetation. In *Remote Sensing of Biosphere Functioning*, edited by R. J. Hobbs and H. A. Mooney. Springer Verlag, New York, pp. 203-219.

Lillesand, T. and R. Kiefer (1994). *Remote Sensing and Image Interpretation, 3rd Edition*. John Wiley & Sons, Inc., New York, pp. 313-318.

Lu, D., P. Mausel, E. Brondizio, and E. Moran (2004). Change detection techniques. *Int. J. Remote Sensing*, 24(12):2365-2407.

Rogan, J., F. Franklin, and D. Roberts (2002). A comparison of methods for monitoring multitemporal vegetation change using Thematic Mapper imagery. *Remote Sensing Env*., 80(1):143-156.

Stow, D. and D. Chen (2002). Sensitivity of multitemporal NOAA AVHRR data of an urbanizing region to land-use/land-cover changes and misregistration. *Remote Sensing Env.*, 80:297-307.

Verbyla, D. and S. Boles (2000). Bias in land cover change estimates due to misregistration. *Int. J. Remote Sensing*, 21(18):3553-3560.

Wang, J., K. Di, and R. Li (2005). Evaluation and improvement of geopositioning accuracy of IKONOS stereo imagery. *J. Surv. Engineering*, 131(2):35-42.